Accepted Manuscript

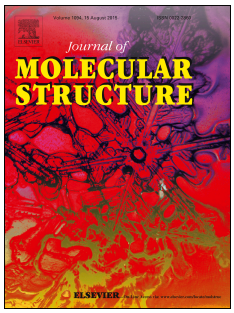

Can C-H···F-C hydrogen bonds alter crystal packing features in the presence of N-H···O=C hydrogen bond?

Hare Ram Yadav, Angshuman Roy Choudhury

PII: S0022-2860(17)31150-X

DOI: 10.1016/j.molstruc.2017.08.083

Reference: MOLSTR 24221

To appear in: *Journal of Molecular Structure*

Received Date: 18 April 2017

Revised Date: 18 August 2017

Accepted Date: 23 August 2017

Please cite this article as: H.R. Yadav, A.R. Choudhury, Can C-H···F-C hydrogen bonds alter crystal packing features in the presence of N-H···O=C hydrogen bond?, *Journal of Molecular Structure* (2017), doi: 10.1016/j.molstruc.2017.08.083.

Can C–H···F–C hydrogen bonds alter crystal packing features in the presence of N–H···O=C hydrogen bond?

Hare Ram Yadav and Angshuman Roy Choudhury*

Department of Chemical Sciences, Indian Institute of Science Education and Research (IISER) Mohali, S. A. S. Nagar Sector 81 Knowledge City, Mohali, Punjab. 140306. India

Abstract

Intermolecular interactions involving organic fluorine have been the contemporary field of research in the area of organic solid state chemistry. While a group of researchers had refuted the importance of "organic fluorine" in guiding crystal structures, others have provided evidences for in favor of fluorine mediated interactions in the solid state. Many systematic studies have indicated that the "organic fluorine" is capable of offering weak hydrogen bonds through various supramolecular synthons, mostly in the absence of other stronger hydrogen bonds. Analysis of fluorine mediated interaction in the presence of strong hydrogen bonds has not been highlighted in detail. Hence a thorough structural investigation is needed to understand the role of "organic fluorine" in crystal engineering of small organic fluorinated molecules having the possibility of strong hydrogen bond formation in the solution and in the solid state. To fulfil this aim, we have synthesized a series of fluorinated amides using 3-methoxyphenylacetic acid and fluorinated anilines and studied their structural properties through single crystal and powder X-ray diffraction methods. Our results indicated that the "organic fluorine" plays a significant role in altering the packing characteristics of the molecule in building specific crystal lattices even in the presence of strong hydrogen bond.

Key words: "Organic fluorine", weak interactions, structural diversity

Introduction

Various supramolecular assemblies in gaseous [1], liquid [2] and solid [3] states of mater are always governed by the non-covalent interactions between the atoms and molecules. Molecular recognition through strong and weak forces in the solid state lay the path for supramolecular chemistry and crystal engineering [4]. A careful control on strong and weak intermolecular interactions allows us to form different molecular assemblies in the solid state. Among the well-studied intermolecular forces, conventional hydrogen bonding (X–H···Y, X,Y= F, O, N etc.) offers stabilization by 15-40 kcal/mole and hence is considered to be the most important intermolecular force in building and controlling the crystal structures of various covalent molecules [3, 5]. Other hydrogen bonds (X–H···Y–C where X = O, N and Y = O, N, S) are also considered as significant in crystal engineering as the stabilization energy associated with such intermolecular forces falls in the range of 4-15 kcal/mole [3]. Weaker intermolecular forces having energy less than 4 kcal/mole include C–H···X (X = O, N, S), X–H···π, (X = C, N, O, S) and π···π interactions [3]. Intermolecular interactions involving halogens have also been recognized to provide directional preferences in building organic supramolecular synthons in the crystal lattice with the stabilization energy <5 kcal/mole [6].

Among the halogens, fluorinated organic molecules find wide applications in the syntheses of drugs, pharmaceutical products, agrochemicals *etc* due to its unique properties [7]. The structural chemistry aspects of fluorinated organic molecules have been the theme of contemporary research. Since the C–F bond is stronger than a C–H bond, majority of the fluorinated compounds are more resistant to metabolic degradation and external affects (temperature) than its non-fluorinated analogue [8]. Our recent efforts and reports from other groups indicate that the intermolecular interactions involving one or more C–F groups in a small molecule offers significant stabilization to crystal packing [9]. Although, the intermolecular interactions involving C–F bond in organic compounds were historically described in the literature as ‘very weak’, ‘van der Waals’ or ‘not so significantly short’ and hence were not categorized among the crystal engineering tools for a long time [10], our results contradicts such belief. In late 90s and later, groups of authors have demonstrated the importance of C–F bond in the solid state chemistry of small organic molecules [11]. It was demonstrated that interactions involving a C–F

group do occur frequently then was predicted earlier [11]. During the last decade it has been demonstrated that fluorine generates different types of packing patterns *via* C–H···F, C–F···F, and C–F··π interactions especially in the absence of strong hydrogen bond donors (N–H, O–H etc) and acceptors (C=O) [12]. Thalladi *et al.* identified four possible types of C–H···F hydrogen bonded synthons (Figure 1) in 1998 [11a].

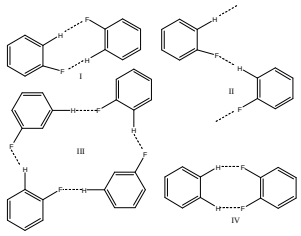

Figure 1: Types of known C–H···F hydrogen bonded synthons. Synthon I, Synthon II, Synthon III and Synthon IV.

Most of the previously reported studies on such C–H···F–C hydrogen bonds have been limited to a selection of compounds where potential strong hydrogen bond donors and acceptors were absent [9a-d]. The role of C–F group in the presence of strong hydrogen bonding has been noted before [12] but the area needs better understanding and insights. Chopra *et al.*, [12a], and Nayak *et al.*, [12b, c], reported crystal structures of a series of benzanilides having halogen substitution at various positions (Figure 2).

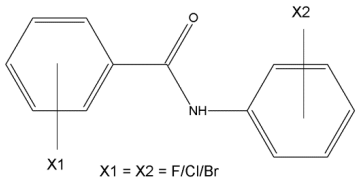

Figure 2: System of benzanilide studied by Chopra *et al.* [12a], and Nayak *et al.* [12b, c]

Their structural analyses with the halogenated benzanilides indicated that although all the crystal structures were highly stabilized by a strong N–H···O=C hydrogen bond (forming molecular chain), the packing characteristics were significantly different based on the identity (F, Cl and Br) and position (*ortho*-, *meta*-, *para*-) of the halogen substitution on the either rings. They have shown that with the change in the nature and position of halogen substitution, several different structural features were generated among the compounds studied by them. Due to the near planarity of all the molecules, the scope for fluorine mediated interactions in the crystal structures were somewhat limited.

Therefore, we wanted to induce better flexibility in the molecule and study the effects of fluorine mediated interactions in a different series of molecules. In the current manuscript, we intend to analyze the crystal structures of eighteen new phenylacetanilides (Figure 3) containing a methoxy group in the phenyl ring originating from the phenylacetic acid and one or two fluorine atoms in the phenyl ring originating from aniline. This molecular framework allows for the torsional flexibility of the molecules due to the incorporation of an additional $–CH_2–$ group in the system, thereby increasing the possibility of occurrence of different fluorine mediated interactions.

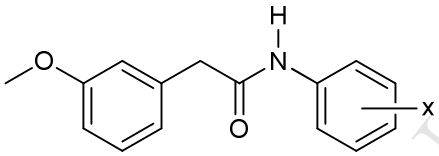

X = mono-F or di-F

Figure 3: System of phenyl acetanilide studied

In these structures, the strong N–H···O=C hydrogen bond is expected to be the key feature and the weaker intermolecular forces such as C–H···F, C–H···O, and C–H··π are expected to play a significant role in altering the molecular conformation and thereby resulting into structural diversity.

Experimental:

All the starting materials were purchased from Sigma-Aldrich and were used without further purification. All the compounds (Scheme 1) were synthesized from their corresponding aniline and 3-methoxyphenylacetic acid initially following the procedure reported by Nagarajan *et al.* [13], and later, on experiencing poor yield of some of our target molecules we followed a different synthetic procedure for better yield with the use of less hazardous chemicals [14]. 3-methoxy-phenyl-acetic acid **1a** (1.0 eqv), fluorine substituted aniline **1b** (1.10 eqv), *N*-(3-Dimethylaminopropyl)-*N′*-ethylcarbodiimide hydrochloride (EDC.HCl) (1.10 eqv) and hydroxybenzotriazole (HOBt) (0.50 eqv) were mixed in a round bottom flask and *N*-methylpyrrolidin-2-one (NMP) solvent was added at room temperature (25 ˚C) under N_2 environment. The reaction mixture was stirred at room temperature for 18 hours. After the reaction was over, water and ethyl acetate were added and the mixture was stirred for 15 mins.

The mixture was then allowed to settle in a separating funnel, and the lower aqueous phase was removed and discarded. The organic phase was washed a few times with water and brine solution to remove the unreacted water-soluble compounds and to achieve better separation of organic and aqueous layers. Then the organic phase was collected over excess anhydrous sodium sulfate to remove traces of moisture in the organic phase. Then the organic solvent was removed under reduced pressure on a rotary evaporator to extract the solid target compound. The crude product was purified by column chromatography using ethyl acetate/hexane mixture as the mobile phase. All the pure compounds were characterized by ^{1}H, ^{13}C and ^{19}F NMR (400 MHz, Bruker Biospin Avance-III NMR spectrometer), FTIR (Perkin Elmer Spectrum 2) and the melting point of all the compounds were determined by differential scanning calorimetry (DSC) (Perkin Elmer Diamond 8000 DSC). All the characterization details (NMR, IR, DSC and PXRD) are provided as electronic supporting information (ESI).

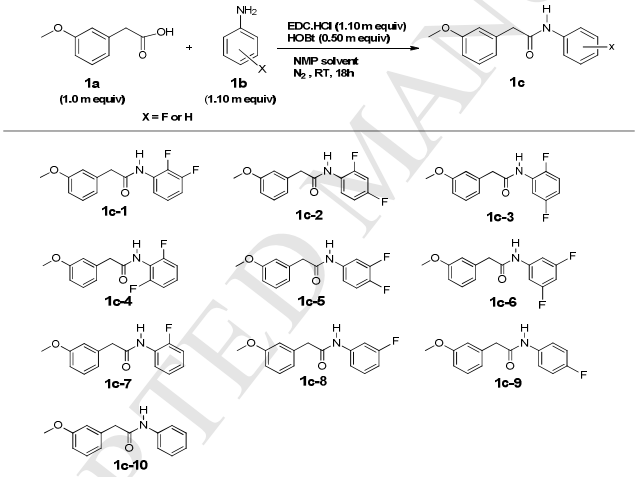

Scheme 1

Powder X-ray Diffraction (PXRD) Analysis

PXRD patterns of all the pure compounds were recorded on a Rigaku Ultima IV diffractometer using parallel beam geometry equipped with a Cu – K_α radiation, 2.5° Primary and secondary solar slits, 0.5° divergence slit with 10 mm height limit slit, sample rotation stage (120 rpm) attachment and DTex Ultra detector. The tube voltage and current applied were 40 kV and 40 mA. The data were collected over an angle range 5 to 50° with a scanning speed of 2° per minute with 0.02° step. The observed PXRD patterns have been compared (using WINPLOTR [15]) with the simulated PXRD patterns generated from the crystal coordinates using Mercury.

Crystal Growth, Single Crystal Data Collection, Structure Solution and Refinement

Single crystals of desired size and quality were grown by slow evaporation by dissolving the compound in different solvents like acetone, methanol, ethanol, ethyl acetate, dichloromethane, acetonitrile, toluene or a mixture of solvents such as DCM/hexane, chloroform/hexane, ethyl acetate/hexane, methanol/hexane and acetone/hexane etc.

Single crystal X-ray diffraction data (Table 1-2) were collected using a Rigaku XtaLABmini X-ray diffractometer equipped with Mercury CCD detector with graphite monochromatic Mo-Kα radiation (λ = 0.71073 Å) at 100.0(2) K using ω scans. The data were reduced using Crystal Clear suite 2.0 [16] and the space group determination was done using Olex2 [17]. The crystal structures were solved by using ShelXL [18] and were refined using ShelXT [19] through Olex2 suite. All the hydrogen atoms were geometrically fixed and refined using the riding model. Absorption correction was done by multi-scan method. Data collection, crystal structure solution and refinement details for all the compounds are listed in the Table 1(a)-(b). All the packing and interaction diagrams have been generated using Mercury 3.5 [20]. Geometric calculations have been done using PARST [21] and PLATON [22].

Computational analysis

The structures of all the molecules were stabilized mostly by strong N–H···O=C and weak C–H···F–C hydrogen bonds. Intermolecular C–H···O hydrogen bonds generally involved the proton connected to sp^3 C atom of the methoxy group. As these C–H···O hydrogen bonds are considered very weak, their contribution in stabilizing the crystal structure is insignificant. The stabilization energy offered by the N–H···O=C and C–H···F–C hydrogen bonds are calculated using Gaussian 09 [23] package, MP2 [24] level of theory and 6-31++(d,p) basis set similar to an earlier report [9d, e]. The single point energy of the dimer (without optimization) and the monomer (without optimization) molecule were calculated using Gaussian09 and the stabilization energy (SEg_{09}) was computed as $SEg_{09} = E_{dimer} - 2 \times E_{monomer}$ starting from the experimentally observed geometry of the dimer and the monomer respectively in their respective crystal structures. The Basis set superposition error (BSSE) was corrected by the counterpoise method [25]. GaussView [26] was used to visualize the molecules during the energy calculations.

Table 1: Single crystal X-ray diffraction data of compounds 1c-1 to 1c-5

Identification code	**1c-1**	**1c-2**	**1c-3**	**1c-4**	**1c-5**
CCDC Number	1540707	1540709	1540710	1540711	1540712
Formula	$C_{15}H_{13}F_2NO_2$	$C_{15}H_{13}F_2NO_2$	$C_{15}H_{13}F_2NO_2$	$C_{15}H_{13}F_2NO_2$	$C_{15}H_{13}F_2NO_2$
Formula weight	277.26	277.26	277.26	277.26	277.26
Crystal system	Monoclinic	Monoclinic	Monoclinic	Monoclinic	Monoclinic
Space group	$P2_1/c$	$P2_1/c$	$P2_1/c$	$C2/c$	$P2_1/c$
a (Å)	11.6788(17)	10.9903(6)	11.0509(16)	22.3996(16)	5.8400(12)
b (Å)	4.8674(7)	4.6917(2)	12.231(3)	4.7464(4)	26.820(5)
c (Å)	27.251(4)	28.1963(13)	9.4633(17)	25.2796(16)	10.960(2)
β (°)	124.699(9)	118.451(3)	96.740(7)	103.356(4)	131.45(3)
V (Å^3)	1273.6(3)	1278.30(11)	1270.2(4)	2615.0(3)	1286.7(5)
Z	4	4	4	8	4
ρ_{calc} (g cm^{-3})	1.446	1.441	1.450	1.409	1.431
Temperature (K)	100.0	100.0	100.0	100.0	100.0
μ/ mm^{-1}	0.116	0.115	0.116	0.113	0.114
$2\theta_{min,max}$ (°)	3.636 to 50.04	3.92 to 58.26	6.316 to 54.976	3.312 to 56.564	3.038 to 49.8
F(000)	576.0	576.0	576.0	1152.0	576.0
$h_{min,max}$; $k_{min,max}$; $l_{min,max}$;	-13 ,13; -5,4; -31, 32	-15, 14; -5, 6; -38 ,38	-14, 14; -13, 15; -12 ,12	-26, 29; -6, 6; -30, 33	-6, 4; -31, 31; -12, 12
No. of observed reflections	8518	12235	8207	6649	5567
R_{int}	0.0201	0.0539	0.0319	0.0272	0.0486
No. of unique reflections	2242	3454	2892	3235	2189
R_1 [I > 2σ(I)]	0.0366	0.0484	0.0424	0.0447	0.0491
wR_2 (all data)	0.1037	0.1242	0.1203	0.1122	0.1181
GooF	1.043	1.023	1.035	1.016	1.036
$\Delta\rho_{max,min}$/eÅ^{-3}	0.61, -0.28	0.27, -0.25	0.28, -0.26	0.31, -0.36	0.22, -0.29

Table 2: Single crystal X-ray diffraction data of compounds 1c-6 to 1c-10*

Identification code	**1c-6**	**1c-7**	**1c-9**	**1c-10**
CCDC Number	1540713	1540714	1540715	1540708
Formula	$C_{15}H_{13}F_2NO_2$	$C_{15}H_{14}FNO_2$	$C_{15}H_{14}FNO_2$	$C_{15}H_{15}NO_2$
Formula weight	277.26	259.27	259.27	241.28
Crystal system	Monoclinic	Monoclinic	Monoclinic	Monoclinic
Space group	$P2_1/c$	$P2_1/c$	$P2_1/c$	$P2_1/c$
a (Å)	10.989(2)	4.729(3)	5.0169(14)	9.5059(16)
b (Å)	12.176(3)	11.406(5)	12.106(4)	10.8524(17)
c (Å)	9.5202(19)	23.474(12)	20.553(9)	24.154(4)
β (°)	97.740(12)	93.85(2)	95.217(16)	96.267(7)
V (Å^3)	1262.3(5)	1263.4(11)	1243.1(8)	2476.9(7)
Z	4	4	4	8
ρ_{calc} (g cm^{-3})	1.459	1.363	1.385	1.294
Temperature (K)	100.0	100.0	100.0	100.0
μ/ mm^{-1}	0.117	0.100	0.102	0.086
$2\theta_{min,max}$ (°)	6.284 to 55.02	6.324 to 55.056	6.732 to 55.226	6.096 to 50.052
F(000)	576.0	544.0	544.0	1024.0
$h_{min,max}$; $k_{min,max}$; $l_{min,max}$;	-14, 14; -15, 15; -12, 12	-4, 6; -14, 14; -30, 30	-6, 6; -15, 15; -26, 26	-11, 10; -12, 12; -28, 28
No. of observed reflections	13420	11536	8716	17289
R_{int}	0.0532	0.0636	0.0658	0.0700
No. of unique reflections	2905	2889	2833	4332
R_1 [I > 2σ(I)]	0.0478	0.0560	0.0475	0.0594
wR_2 (all data)	0.1239	0.1537	0.1213	0.1505
GooF	1.091	1.056	0.986	1.110
$\Delta\rho_{max,min}$/eÅ^{-3}	0.30, -0.21	0.27, -0.23	0.30, -0.31	0.21, -0.25

*Crystals of **1c-8** could not be grown and hence structure determination was not possible.

Results and discussions

All the compounds reported in this manuscript contains an amide group (–CONH–) therefore all the crystal structures discussed in this manuscript exhibit the strong N–H···O=C hydrogen-bonded chain as a common feature. All the compounds preferred to crystallize in $P2_1/c$ space group except one (**1c-4**) having different unit cell parameters and there were no indication of isostructurality in terms of unit cell parameters among these compounds.

*Structure of the compound 2-(3-methoxyphenyl)-N-(2,3-difluorophenyl)acetamide (**1c-1**):*

In the structure of the compound **1c-1** (Table 1a and Figure 4a), the strong N–H···O=C hydrogen bond is responsible for the formation of one-dimensional catameric chain along the crystallographic *b* direction (Figure 4b, Table 3) with all the molecules aligned in parallel (↑↑↑↑) orientation (Figure 4b). Although there are two fluorine atoms i.e. F1 and F2 corresponding to *ortho*- and *para*- positions but none of these fluorine atoms participated in the C–H···F hydrogen bond with any of the available aromatic protons and hence there is no significant contribution of fluorine in crystal packing. Two parallel molecular chains of strong N–H···O=C hydrogen bonds are itself connected by C4–H4···O2 hydrogen bond (Figure 4c). Carbonyl oxygen is also participate in the formation of dimer synthon *via* inversion center symmetry by utilization of C15–H15···O1 hydrogen bond. The shortest F···F distance (3.002(2)) observed is also beyond the sum of the van der Waals' radii of the interacting F atoms.

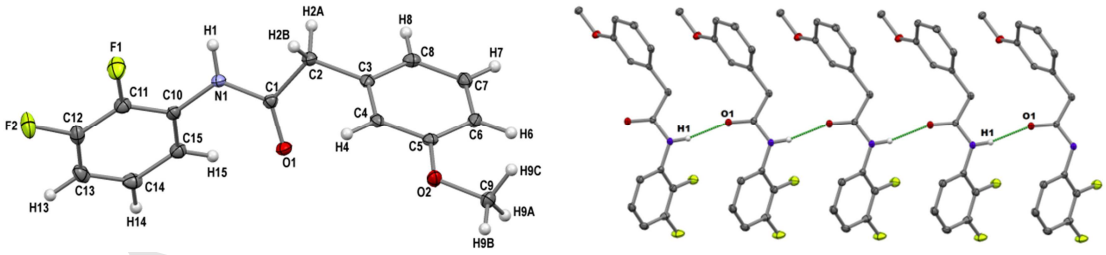

(a) **(b)**

Figure 4: (a) ORTEP of **1** drawn with 50% ellipsoidal probability, **(b)** N1–H1···O1 Hydrogen bond in one-dimensional catameric chain along *b*-axis.

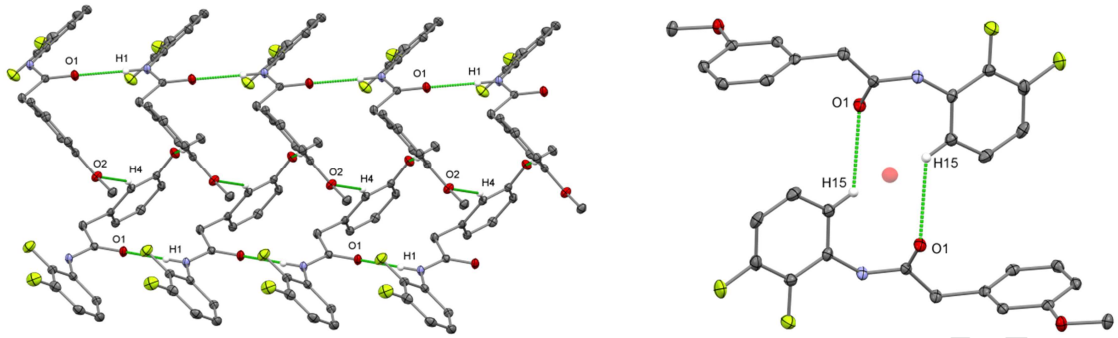

(c) **(d)**

Figure 4: (c) Two parallel N1–H1···O1 Hydrogen bond chain interconnected by C4–H4···O2 hydrogen bond. **(d) A** dimer synthon *via* inversion center symmetry by utilization of C15–H15···O1 hydrogen bond.

Table 3: Intermolecular interactions in 1c-1

D–H···A/(Å)	(D···H)/Å	D(D···A)/Å	d(H···A)/Å	∠D–H···A/°	SYMMETRY	SE_{g09} (kcal/mol)
N1–H1···O1	1.030	2.976(2)	1.97	164	x, y - 1, z	-143
C4–H4···O2	1.080	3.374(3)	2.38	153	1 - x, y - ½, $^3/_2$ - z	-5.4
C15–H15···O1	1.080	3.380(2)	2.60	129	- x, 1- y, 1- z	-7.1

*Structure of 2-(3-methoxyphenyl)-N-(2,4-difluorophenyl)acetamide (**1c-2**)*

In the structure of the compound **1c-2** (Figure 5a) strong hydrogen N1–H1···O1 bond propagates along the *b* axis with all the molecules aligned in parallel (↑↑↑↑) orientation (Figure 5b, Table 4) as was seen in **1c-1**. Two parallel N1–H1···O1 Hydrogen bond chain itself interconnected by C4–H4···O2 hydrogen bond.Fluorine atoms were not involved in any C–H···F hydrogen bond.

Table 4: Intermolecular interactions in 1c-2

D–H···A/(Å)	(D···H)/Å	D(D···A)/Å	d(H···A)/Å	∠D–H···A/o	SYMMETRY	SE_{g09} (kcal/mol)
N1–H1···O1	1.030	2.806(2)	1.85	154	x, y - 1, z	-138
C4–H4···O2	1.080	3.510(3)	2.62	139	1 - x, ½ - y, $^3/_2$ - z	-5.8

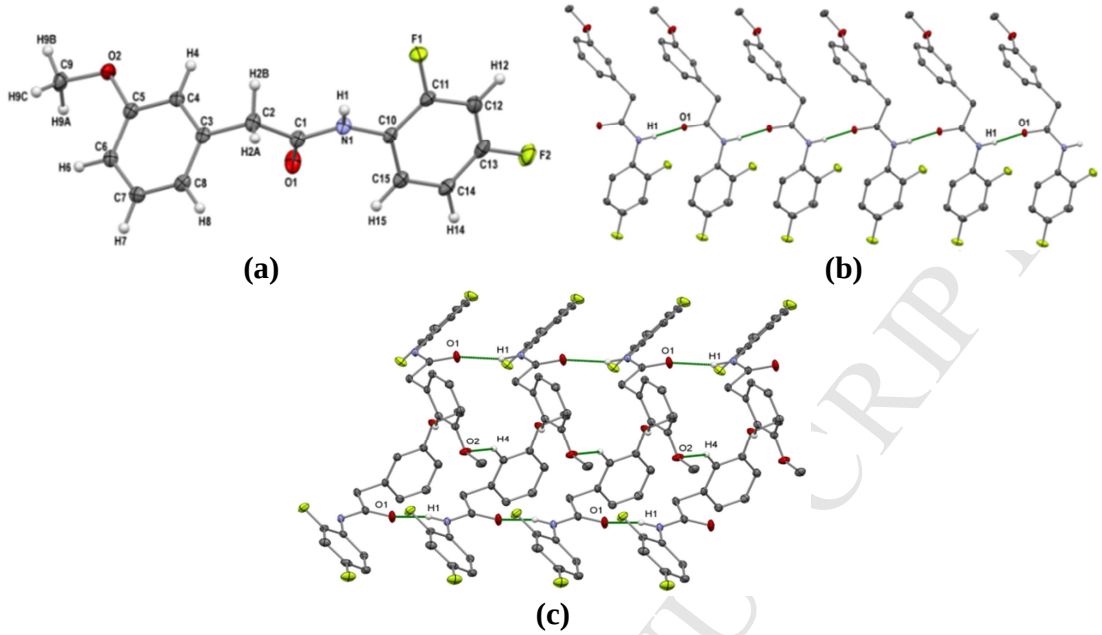

Figure 5: (a) ORTEP of **1c-2** drawn with 50% ellipsoidal probability, **(b)** Strong N1–H1···O1 Hydrogen bond and C2–H2A···π interaction in one-dimensional catameric chain along *b*-axis and bond both are parallel. **(c)** Two parallel N1–H1···O1 Hydrogen bond chain interconnected by C4–H4···O2 hydrogen bond.

*Structure of N-(2,5-dichlorophenyl)-3-methoxyphenylacetamide (**1c-3**)*

Compound **1c-3** (Figure 6a) mainly displays three types of interactions have been found, N–H···O, C-H···O and C–H···F hydrogen bonds. Strong N–H···O hydrogen bond is responsible for the formation of one-dimensional infinite catameric chain with molecules arranged in anti-parallel (↑↓↑↓↑↓) orientation along the crystallographic *c* direction (Figure 6b, Table 5).

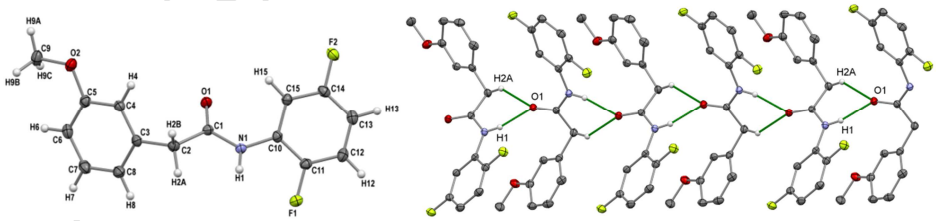

Figure 6: (a) ORTEP of **1c-3** drawn with 50% ellipsoidal probability, **(b)** Strong N1–H1···O1 Hydrogen bond generating one-dimensional alternate antiperiplanar infinite catameric chain along *c*-axis.

Ortho-fluorine (F1) of amine ring is found to act as a bifurcated acceptor. The hydrogen bond involving C13–H13···F1 and C7–H7···F2 leads to the formation 2-dimentional net-like structure (Figure 6c). Further, through C12–H12···F1 hydrogen bond, centrosymmetric dimers have been identified. These dimers are once again connected to each other by C7–H7···F2 hydrogen bond forming a ribbon-like structure (Figure 6d).

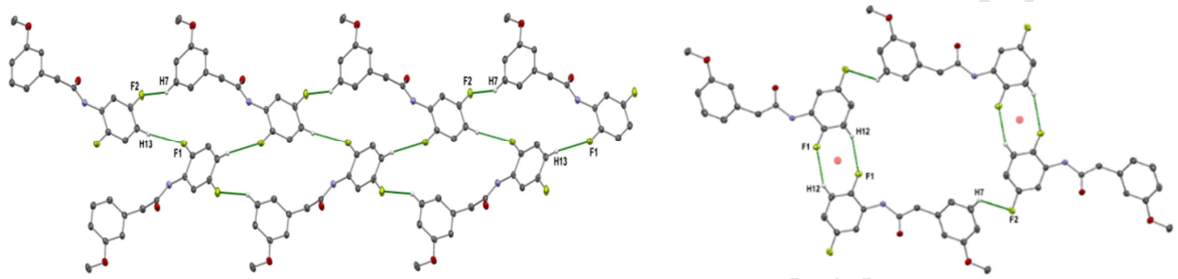

(c) **(d)**

Figure 6: (c) a 2-dimentional sheet-like structure **(d)** head to head 8-membered supramolecular synthon in which aromatic C–H···F interactions are involved (a dimer form).

Table 5: Intermolecular interactions in 1c-3

D–H···A/(Å)	(D···H)/Å	D(D···A)/Å	d(H···A)/Å	∠D–H···A/°	SYMMETRY	SE_{g09} (kcal/mol)
N1–H1···O1	1.030	2.876(1)	1.87	166	x, ½ -y , ½ +z	-12.1
C2–H2A···O1	1.080	3.236(2)	2.32	142		
C7–H7···F2	1.080	3.294(2)	2.56	124	x, y -1, z	-1.3
C12–H12···F1	1.080	3.380(2)	2.46	143	1-x, 1-y, -z+2	-2.7
C13–H13···F1	1.080	3.602(2)	2.53	170	1-x, y+ ½, $^3/_2$-z	-2.8

*Structure of 2-(3-methoxyphenyl)-N-(2,6-difluorophenyl)acetamide (**1c-4**)*

The molecules of the compound **1c-4** (Figure 7a) are found to form catameric chain along the *b* direction involving N1–H1···O1 hydrogen bond (Figure 7b, Table 6) in parallel (↑↑↑↑) orientation. Weak C2–H2···π interactions (2.88 Å), are also observed here in this molecular chain (Figure 7b).

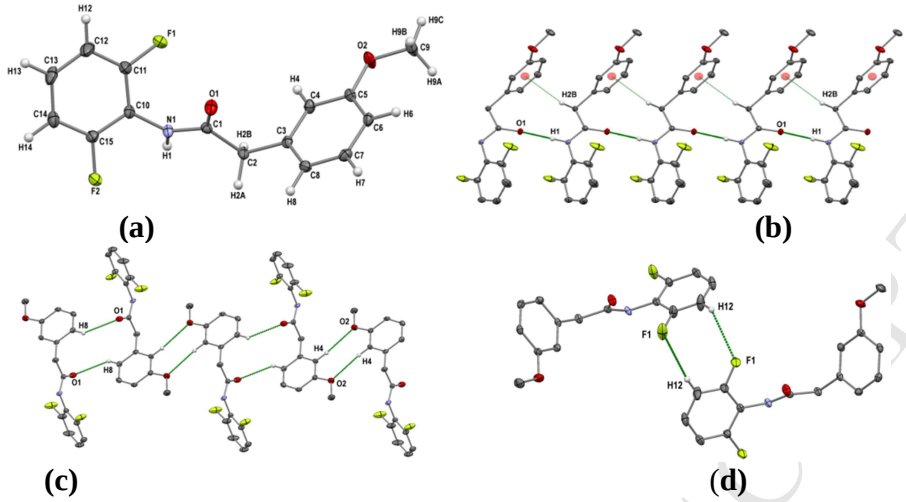

Figure 7: (a) ORTEP of **1c-4** drawn with 50% ellipsoidal probability, **(b)** Strong N1–H1···O1 Hydrogen bond and aromatic C–H···π interactions both parallel generating one-dimensional infinite catameric chain along *b*-axis. **(c)** Two different type of homo synthon *via* inversion center by utilization of C–H···O hydrogen bond and creating a tap like structure. **(d)** C12–H12···F1 hydrogen bond that generate 8-member non-planar supramolecular synthon.

Both *ortho*- hydrogens of the methoxyphenyl ring are individually involved in two different C–H···O hydrogen bonds *via* inversion center. The carbonyl oxygen is the acceptor in one hydrogen bond while the oxygen of the methoxy group in another is acting as the acceptor thereby generating a ribbon-like structure (Figure 7c). The *m*-hydrogen (H12) of the aniline ring forms a dimer through a very weak C–H···F hydrogen bond (∠C12–H12···F1 = 125°) involving F1, and that second fluorine (F2) does not participate in any type of interactions (Figure 7d).

Table 6: Intermolecular interactions in 1c-4

D–H···A/(Å)	(D···H)/Å	D(D···A)/Å	d(H···A)/Å	∠D–H···A/°	SYMMETRY	SE_{g09} (kcal/mol)
N1–H1···O1	1.030	2.767(2)	1.75	167	x, 1+y, z	-13.8
C2–H2B···π	1.080	3.499	2.92	118	x, y -1, z	
C8–H8···O1	1.080	3.417(2)	2.58	134	½ -x, ½ -y, 1+z	-6.7
C4–H4···O2	1.080	3.598(2)	2.56	160	1-x, 1-y, 1-z	-3.1
C12–H12···F1	1.080	3.384(2)	2.65	125	1-x, y, $^3/_2$-z	-2.4

*Structure of 2-(3-methoxyphenyl)-N-(3,4-difluorophenyl)acetamide (**1c-5**)*

This compound **1c-5** (Figure 8a), unlike other amides discussed above, the carbonyl oxygen is found to act as a bifurcated acceptor (Figure 8b, Table 7). In addition to the bifurcated hydrogen bonds (N1–H7···O1 and C8–H8···O1), weak C7–H7···F1 hydrogen bonds are also identified in the same synthon (Figure 8b). Herein the molecules are arranged in the opposite directions (↑↓↑↓↑↓). A zig-zag molecular chains are formed by C14–H14···O2 hydrogen bond offered by methoxy oxygen via *c*-glide symmetry (Figure 8c).

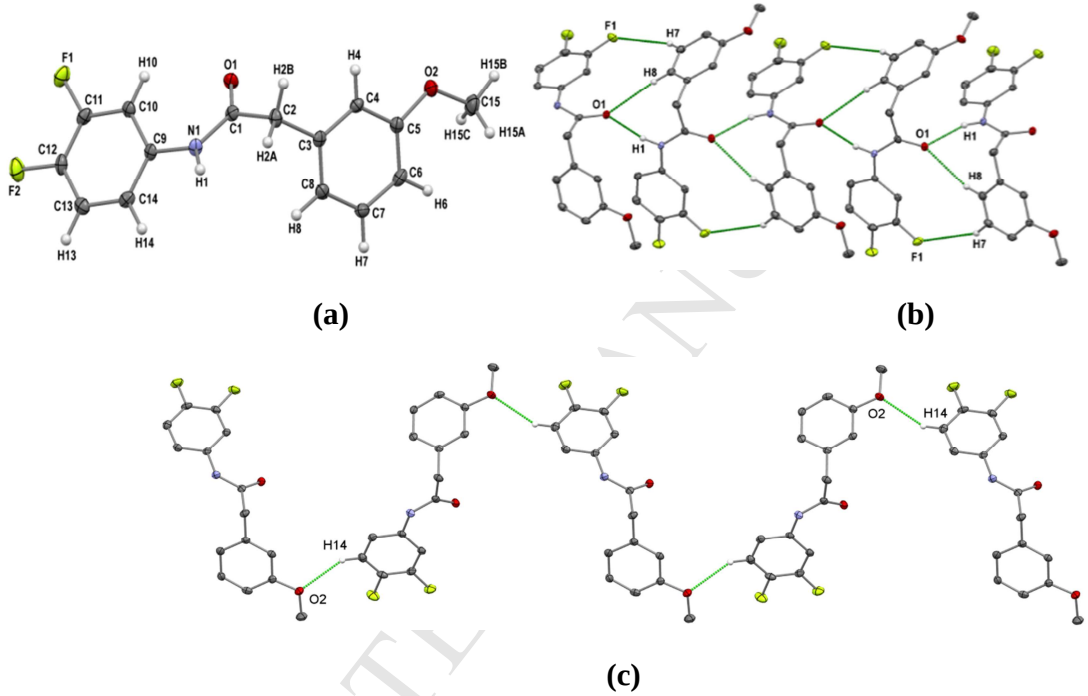

Figure 8: (a) ORTEP of **1c-5** drawn with 50% ellipsoidal probability, **(b)** Strong N1–H1···O1 Hydrogen bond along with weak C7–H7···F1 and C8–H8···O1 hydrogen bonds in one dimensional catameric chain type structure. **(c)** A zig-zag molecular chain offered by methoxy oxygen via *c*-glide symmetry.

Table 7: Intermolecular interactions in 1c-5

D–H···A/(Å)	(D···H)/Å	D(D···A)/Å	d(H···A)/Å	∠D–H···A/°	SYMMETRY	SE_{g09} (kcal/mol)
N1–H1···O1	1.030	2.828(3)	1.88	152	x-1, $^{1}/_{2}$-y, z-$^{1}/_{2}$	-13.3
C8–H8···O1	1.080	3.531(3)	2.58	147		
C7–H7···F1	1.080	3.624(3)	2.68	145		
C14–H14···O2	1.080	3.307(3)	2.34	148	x-2, -y+$^{1}/_{2}$, z-$^{1}/_{2}$	-2.9

Structure of 2-(3-methoxyphenyl)-N-(3,5-difluorophenyl)acetamide (1c-6)

Compound **1c-6** (Figure 9a) also has molecular chains involving N1–H1···O1, C2–H2A···O1 and C8–H8···F1 hydrogen bonds just as was seen in **1c-5** (Figure 9b, Table 8) though the unit cell parameters are different for **1c-5** and **1c-6**. The molecules in this chain are arranged in the opposite directions (↑↓↑↓↑↓) like **1c-3** and **1c-4**. Like the compound **1c-3**, this molecule also forms a symmetrical 8-membered dimer by the utilization of C15–H15···F2 hydrogen bonds (Figure 9c). The F1 group also involved in the formation of molecular chain by C7–H7···F1 hydrogen bonds *via* translational symmetry along *b*-axis (Figure 9d).

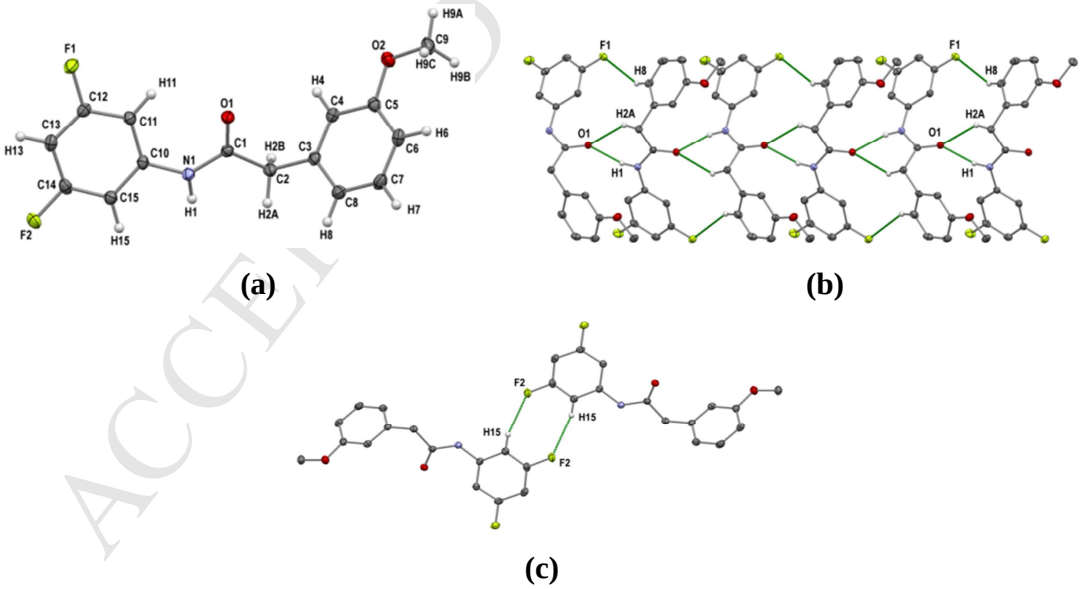

Figure 9: (a) ORTEP of **1c-6** drawn with 50% ellipsoidal probability, **(b)**: Strong N–H···O hydrogen bond and weak C8–H8···F1 hydrogen bond involved in formation of one-dimensional band like structure in crystal packing. **(c)** Inversion center related 8-member head to head supramolecular homo synthon.

Table 8: Intermolecular interactions in 1c-6

D–H···A/(Å)	(D···H)/Å	D(D···A)/Å	d(H···A)/Å	∠D–H···A/°	SYMMETRY	SE_{g09} (kcal/mol)
N1–H1···O1	1.030	2.879(2)	1.89	161	x, ½ -y, ½ +z	-13.7
C2–H2A···O1	1.080	3.282(2)	2.39	139		
C8–H8···F1	1.080	3.455(2)	2.52	145		
C7–H7···F1	1.080	3.358(2)	2.61	125	x, y-1, z	-1.3
C15–H15···F2	1.080	3.448(2)	2.40	163	1-x, 1-y, 2-z	-2.9

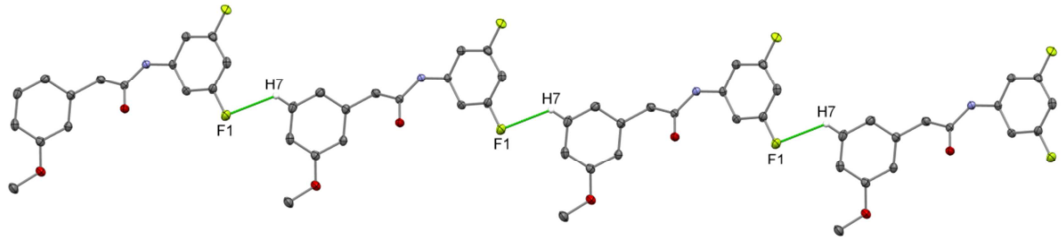

Figure 9: (d) A molecular chain by C7–H7···F1 hydrogen bonds *via* translational symmetry along *b*-axis.

*Structure of 2-(3-methoxyphenyl)-N-(2,-fluorophenyl)acetamide (**1c-7**)*

This mono-fluorinated acetamide (**1c-7**) (Figure 10a) also displays strong N–H···O hydrogen bond along the *a* axis forming an infinite chain with molecules packed in parallel (↑↑↑) orientation *via* translational symmetry only (Figure 10b, Table 9).

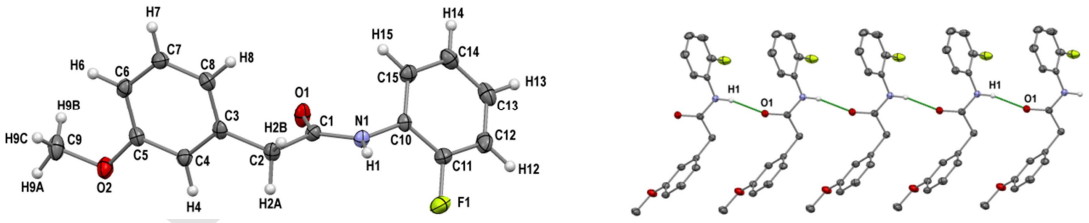

(a) **(b)**

Figure 10: (a) ORTEP of **1c-7** drawn with 50% ellipsoidal probability, **(b)** A symmetrical one-dimensional linear chain of strong N1–H1···O1 hydrogen bond along a-axis.

Simultaneously with the strong hydrogen bond, 4 molecules are connected by weak C–H···O hydrogen bonds and generate a tetramer in which methoxy oxygen behave as a bifurcated

acceptor and this tetrameric unit propagates in a direction perpendicular to the strong hydrogen bond i.e. in the *b* direction (Figure 10c). In addition, the o*rtho*- fluorine and *meta*- hydrogen participates in the formation of a centrosymmetric 8 membered dimer through C12–H12···F1 hydrogen bond (Figure 10d).

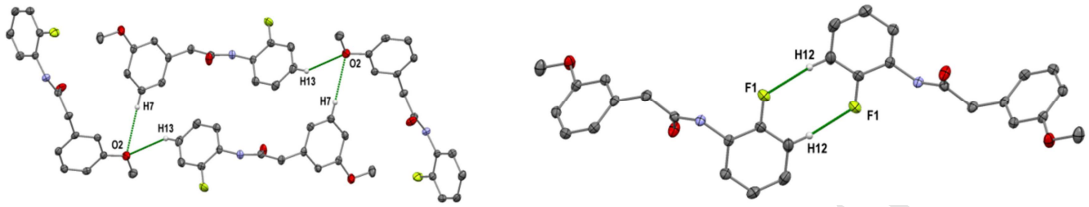

(c) **(d)**

Figure 10: (c) A tetramer synthon unit held by bifurcated C–H···O hydrogen bond, **(d)** Inversion center related 8-member head to head supramolecular homo synthon via C12–H12···F1 hydrogen bond.

Table 9: Intermolecular interactions in 1c-7

D–H···A/(Å)	(D···H)/Å	D(D···A)/Å	d(H···A)/Å	∠D–H···A/o	SYMMETRY	SE_{g09} (kcal/mol)
N1–H1···O1	1.030	2.856(3)	1.86	164	1-x, y, z	-14.0
C13–H13···O2	1.080	3.585(3)	2.62	149	x, ½ -y, ½ +z	-2.2
C7–H7···O2	1.080	3.609(3)	2.53	174	2-x, ½ +y, ½ -z	-4.1
C12–H12···F1	1.080	3.393(3)	2.50	140	1-x, -y, 1-z	-1.8

*Structure of 2-(3-methoxyphenyl)-N-(4,-fluorophenyl)acetamide (**1c-9**)*

Compound **1c-9** (Figure 11a) packs *via* strong N–H···O hydrogen bond propagating along *a*-axis (Figure 11b, Table 10). Two molecules are found to form a *head-to-tail* dimer through C8–H8···F1 hydrogen bond (Figure 11c). Since the fluorine behaves as a bifurcated acceptor here, it also forms a zig-zag chain by C4–H4···F1 hydrogen bond by c-glide (Figure 11d).

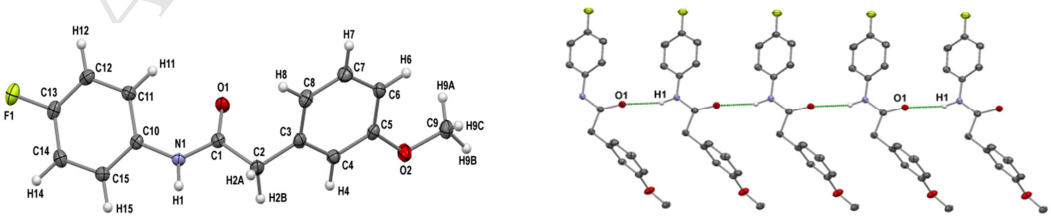

(a) **(b)**

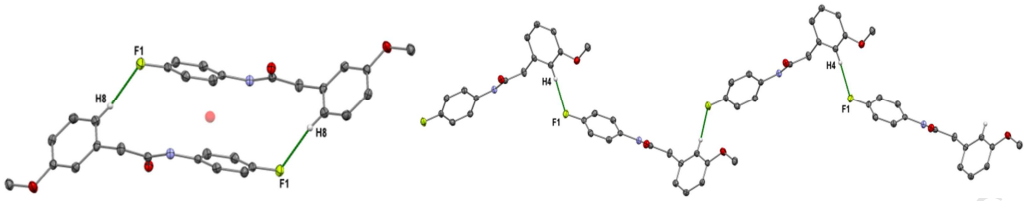

(c) **(d)**

Figure 11: (a) ORTEP of **1c-9** drawn with 50% ellipsoidal probability, **(b)** A symmetrical one-dimensional linear chain of strong N1–H1···O1 hydrogen bond along a-axis. **(c)** Inversion center related dimer synthon through the C8–H8···F1 hydrogen bond **(d)** C4–H4···F1 hydrogen bond in zig-zag chain.

Table 10: Intermolecular interactions in 1c-9

D–H···A/(Å)	(D···H)/Å	D(D···A)/Å	d(H···A)/Å	∠D–H···A/°	SYMMETRY	SE_{g09} (kcal/mol)
N1–H1···O1	1.030	2.897(2)	1.94	154	1+x, y, z	-13.6
C12–H12···O1	1.080	3.531(2)	2.60	144	1-x, 1-y, 1-z	-4.5
C14–H14···O2	1.080	3.631(2)	2.60	152	1+x, $^{3}/_{2}$-y, ½ -z	-1.3
C4–H4···F1	1.080	3.367(2)	2.29	175	x, $^{3}/_{2}$-y, ½ +z	-1.4
C8–H8···F1	1.080	3.380(2)	2.38	154	2-x, 1-y, 1-z	-5.9

*Structure of 2-(3-methoxyphenyl)-N-phenylacetamide (**1c-10**):*

The non-fluorinated compound **1c-10** (Figure 12a) has two molecules (A and B) in the asymmetric unit and they differ in their conformation. The torsion angle between the –CONH– group and the –NPh ring are 54° and 33° respectively. These two crystallographically independent molecules are connected by strong N–H···O hydrogen bond and weak aromatic C–H···π interactions (Figure 12b, Table 11). Interestingly, the two molecules of the asymmetric unit pack in the lattice by ···A···B···A···B···A···B··· fashion through strong N–H···O hydrogen bonds (Figure 12c). This is a unique feature, which was not observed in any of the fluorinated molecules discussed before.

Table 11: Intermolecular interactions in 1c-10

D–H···A/(Å)	(D···H)/Å	D(D···A)/Å	d(H···A)/Å	∠D–H···A/°	SYMMETRY	SE_{g09} (kcal/mol)
N1–H1···O3	1.030	2.855(3)	1.83	173	x, y, z	-14.5
N2–H2···O1	1.030	2.861(3)	1.88	158	x-1, y, z	-14.1
C6–H6···O1	1.080	3.473(3)	2.49	150	2-x, ½ +y, ½ -z	-4.4
C7–H7···O2	1.080	3.573(3)	2.50	170		
C13–H13···O2	1.080	3.430(3)	2.48	146	x, ½ -y, ½ +z	-2.0
C28–H28···O4	1.080	3.472(3)	2.47	154	x, ½ -y, ½ +z	-0.4
C22–H22···O4	1.080	3.467(3)	2.40	168	1-x, ½ +y, ½ -z	-4.0
C27–H27···O3	1.080	3.520(3)	2.59	143	1-x, 1-y, 1-z	-6.7

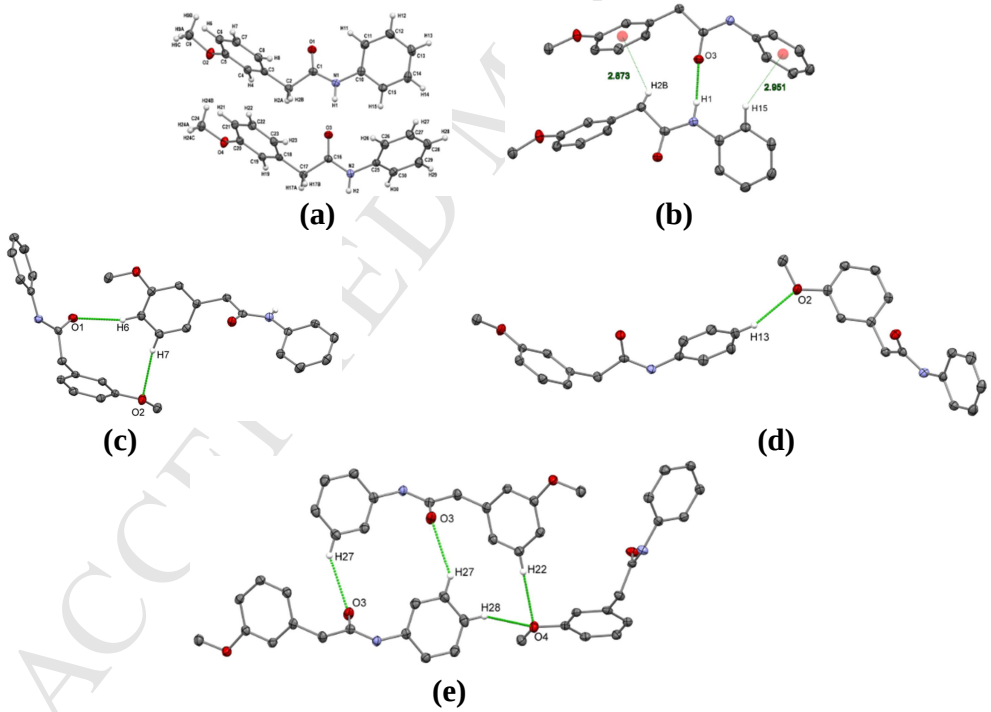

Figure 12: (a) ORTEP of **1c-10** drawn with 40% ellipsoidal probability with atom numbering scheme, **(b)** two molecules of the asymmetric unit with different conformations are connected by strong hydrogen bond and weak C–H···π interactions, **(c)** weak hydrogen bonded dimer involving C–H···O hydrogen bond bonds through carbonyl and methoxy groups, (d) C–H···O

hydrogen bond bonded chain involving methoxy group, (e) C–H···O hydrogen bond bonded motif through carbonyl and methoxy groups.

All the structures reported above indicate that strong N–H···O=C hydrogen bond generally governs the crystal structures of these amides in cooperation with weaker C–H···F–C and C–H···O hydrogen bonds and C–H···π(C_g) interactions. It is well-known in the literature that the amide linkage can result into two types of hydrogen bonded synthons, namely dimer and chain (Scheme 2).

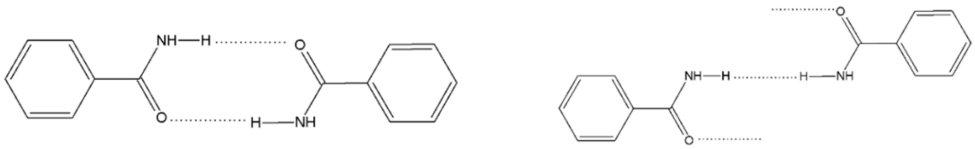

Amide Dimer Amide Chain

Scheme 2

A recent search in the database (CSD, 2017) revels that among the structures reported in the latest version of CSD that there are 3742 hits having the dimer synthon and 7712 hits having the chain synthon. The dimers are mostly formed in cases where the amide is a part of a ring or having –CONHR moiety with R = H, $–CH_3$, $–C_2H_5$ groups. The formation of chain is preferred for molecules having two bulky groups attached to either side of the –CONH– group as is also observed in the structures reported herein. From the crystal data tables (Table 1 and Table 2), it is evident that the non-fluorinated analogue (**1c-10**) has the lowest density (1.295 g/cm^3) compared to the corresponding fluorinated analogues. The density of the difluorinated molecules are in the range between 1.459 g/cm^3 (max) and 1.409 g/cm^3 (min), while that for the two mono-fluorinated compounds are 1.385 g/cm^3 and 1.363 g/cm^3. Although the structure of 1c-10 is stabilized by strong N–H···O=C hydrogen bond in combination with many weak C–H···O hydrogen bonds, the corresponding fluorinated molecules pack better in the lattice thereby resulting into higher density of the compounds. The most striking feature of these hydrogen bonded structures reported in this manuscript is that the weaker C–H···F–C hydrogen bonds are forcing the molecules to pack differently [↑↑↑↑ directions of molecules compared to ↑↓↑↓↑↓ direction of the molecules] in the lattice. Because of such alteration, the unit cell parameters of these compounds are different though the space groups of all the structures (except one) were

same ($P2_1/c$). It is interesting to observe that these compounds did not display polymorphism although there were possibilities of different molecular arrangements keeping the strong hydrogen bond unaltered. The molecular conformation of the compounds reported here are significantly different (Table 12). The orientations of the aromatic rings (C3-C8 and C10-C15) are significantly different in these 9 molecules thereby allowing the fluorine atoms to get involved in different C–H···F–C hydrogen bonds.

Table 12: Torsion angle in (^{0}) of the crystal structures

Compounds	Torsion Angle C4-C3-C2-C1	Torsion Angle C3-C2-C1-O1	Torsion Angle O1-C1-N1-C10	Torsion Angle C11-C10-N1-C1
1c-1	-70	1	5	137
1c-2	-97	-3	2	140
1c-3	-74	32	6	-157
1c-4	-86	-13	-1	57
1c-5	104	-69	0	-28
1c-6	-74	26	4	25
1c-7	98	-20	2	-125
1c-9	-113	14	-2	-31
1c-10	103	-25	3	33

In addition to C–H···F–C hydrogen bonds, many C–H···O hydrogen bonds involving both C=O and $–OCH_3$ groups have been observed in these structures. The stabilization energy offered by C–H···O=C hydrogen bonds are higher than those offered by C–H···OCH_3 hydrogen bonds, which are comparable to those offered by C–H···F–C hydrogen bonds in general. Supramolecular synthons involving 8 members (Scheme 2) forming a dimer through a pair of C–H···F–C hydrogen bonds have been a common feature in these structures. These dimers have been found to be interconnected to each other by another C–H···F–C hydrogen bonds just like the known cases with strong hydrogen bonds involving carboxylic acid dimers. Therefore, it is evident that “organic fluorine” is also capable of acting as hydrogen bond acceptor and can behave in the same manner like other good hydrogen bond acceptors. It is noteworthy that the PXRD patterns, simulated from the single crystal X-ray diffraction data using Mercury, were found to match with the experimental PXRD pattern of the compound concerned, indicating that the bulk phase and the single crystals studied were same. The comparison of the experimental and simulated PXRD patterns are provided in the supporting information.

Conclusions

The structural analysis of this series of fluorinated 2-(3-methoxyphenyl)-N-phenylacetamide derivatives invokes that although the structures of all these compounds are generated by strong hydrogen bonds, several weaker hydrogen bonds together are responsible for altering the molecular packing in the lattice. Different weak C–H···F–C hydrogen bonds immensely influences the crystal structures of these molecules and C–H···π(C_g) interactions together. While strong hydrogen bonds are responsible for the formation of one dimensional molecular chains, the weaker hydrogen bonds involving "organic fluorine" are seen to form chains, dimers, tetramers *etc.* in the crystal lattice. It is also noted that the presence of several weaker interactions has resulted into different unit cell dimensions for these molecules though the unit cell volume remains similar. Therefore, it may be concluded that the influence of many weak hydrogen bonds involving "organic fluorine", which was earlier neglected by Glusker [10a], Dunitz [10c,d], and Howard [10b], is highly significant in altering the crystalline architecture even in the presence of other strong and weak hydrogen bonds.

Acknowledgements

The authors thank IISER Mohali for funding, infrastructural facility, all the instrumental facilities including NMR, FTIR, XtaLABmini X-ray diffractometer, DSC and computational facility etc. HRY Thanks IISER Mohali for research fellowship.

References:

[1] (a) M. Goswami, J.L. Neill, M. Muckle, B.H. Pate, E. Arunan, The J. Chem. Phys. 139 (2013) 104303;

(b) M. Goswami, E. Arunan, Physical Chemistry Chemical Physics 13 (2011) 14153-14162.

[2] (a) S.K. Gupta, S. Setia, S. Sidiq, M. Gupta, S. Kumar, S.K. Pal, RSC Adv. 3 (2013) 12060-12065;

(b) A. Agarwal, S. Sidiq, S. Setia, E. Bukusoglu, J.J. de Pablo, S.K. Pal, N.L. Abbott, Small 9 (2013) 2785-2792.

[3] G.R. Desiraju, T. Steiner, The weak hydrogen bond: in structural chemistry and biology, Oxford University Press on Demand2001.

[4] G.R. Desiraju, Angew. Chem. Int. Ed. Engl. 34 (1995) 2311-2327.

[5] (a) G.A. Jeffrey, An introduction to hydrogen bonding, Oxford university press New York 1997; (b) S. Scheiner, Hydrogen bonding: a theoretical perspective, Oxford University Press 1997;

(c) T. Steiner, Angew. Chem. Int. Ed. Engl. 41 (2002) 48-76.

[6] (a) G. Cavallo, P. Metrangolo, R. Milani, T. Pilati, A. Priimagi, G. Resnati, G. Terraneo, Chem. Rev., 116 (2016) 2478–2601;

(b) L.C. Gilday, S.W. Robinson, T.A. Barendt, M.J. Langton, B.R. Mullaney, P.D. Beer; Chem. Rev., 115 (2015) 7118–7195;

(c) C.B. Aakeröy, P.D. Chopade, J. Desper, Cryst. Growth Des., 13 (2013) 4145–4150;

(d) C.B. Aakeröy, C.L. Spartz, S. Dembowski, S. Dwyre, J. Desper, IUCrJ 2 (2015) 498–510.

[7] (a) A.D. Westwell, Fluorinated Pharmaceuticals: Advances in Medicinal Chemistry, Future Science Ltd London, UK, July 2015;

(b) D. Barnes-Seeman, J. Beck, C. Springer, Curr Top Med Chem. 14 (2014) 855-64.

(c) E.P. Gillis, K.J. Eastman, M.D. Hill, D.J. Donnelly, N.A. Meanwell. J. Med. Chem., 58 (2015) 8315–8359;

(d) T. Fujiwaraa, D. O'Hagan, J. Fluorine Chem. 167 (2014) 16-29;

(e) Organofluorine Chemistry Principles and Commercial Applications Eds. R. E. Banks, B.E. Smart, J.C. Tatlow, Springer, 1994.

[8] (a) G. Valero, X. Companyó, R. Rios, Chem. Eur. J. 17 (2011) 2018-2037;

(b) N.H. Campbell, D.L. Smith, A.P. Reszka, S. Neidle, D. O'Hagan, Org. Biomol. Chem. 9 (2011) 1328-1331.

[9] (a) G. Kaur, P. Panini, D. Chopra, A. Roy Choudhury, Cryst. Growth Des. 12 (2012) 5096-5110;

(b) M. Karanam, A.R. Choudhury, Cryst. Growth Des. 13 (2013) 4803-4814;

(c) E. D'Oria, J.J. Novoa, CrystEngComm 10 (2008) 423-436;

(d) G. Kaur, A.R. Choudhury, Cryst. Growth Des. 14 (2014) 1600-1616;

(e) G. Kaur, A.R. Choudhury, CrystEngComm 17 (2015) 2949-2963;

(f) G. Kaur, S. Singh, A. Sreekumar, A.R. Choudhury, J. Mol. Struct. 1106 (2016) 154-169.

[10] (a) L. Shimoni, J.P. Glusker, Struct. Chem. 5 (1994) 383-397;
(b) J.A. Howard, V.J. Hoy, D. O'Hagan, G.T. Smith, Tetrahedron 52 (1996) 12613-12622;
(c) J.D. Dunitz, R. Taylor, Chem. Eur. J. 3 (1997) 89-98;
(d) J. Dunitz, W.B. Schweizer, Chem. Eur. J. 12 (2006) 6804-6815.

[11] (a) V.R. Thalladi, H.-C. Weiss, D. Bläser, R. Boese, A. Nangia, G.R. Desiraju, J. Am. Chem. 120 (1998) 8702-8710;
(b) A. Choudhury, U. Urs, T.G. Row, K. Nagarajan, J. Mol. Struct. 605 (2002) 71-77;
(c) A. Choudhury, K. Nagarajan, T.G. Row, Cryst. Eng. 6 (2003) 43-55;
(d) A.R. Choudhury, T.N. Guru Row, Cryst. Growth Des. 4 (2004) 47-52;
(e) A.R. Choudhury, T.N.G. Row, CrystEngComm 8 (2006) 265-274;
(f) V. Vasylyeva, K. Merz, Cryst. Growth Des. 10 (2010) 4250-4255.

[12] (a) D. Chopra, T.G. Row, CrystEngComm 10 (2008) 54-67;
(b) S.K. Nayak, M.K. Reddy, D. Chopra, T.N.G. Row, CrystEngComm 14 (2012) 200-210;
(c) S.K. Nayak, M.K. Reddy, T.N. Guru Row, D. Chopra, Cryst. Growth Des. 11 (2011) 1578-1596.

[13] K. Nagarajan, P.K. Talwalker, C.L. Kulkarni, Ind. J. Chem. 24B (1985) 83-97.

[14] L.C. Chan, B.G. Cox, J. Org. Chem. 72 (2007) 8863-8869.

[15] Roisnel T.; Rodriguez-Carvajal, J. WinPLOTR: a Windows tool for powder diffraction patterns analysis Materials Science Forum, Proceedings of the Seventh European Powder Diffraction Conference (EPDIC 7), 2000, 118-123.

[16] CrystalClear2.0, Rigaku Corporation, Tokyo, Japan.

[17] O.V. Dolomanov, L.J. Bourhis, R.J. Gildea, J.A. Howard, H. Puschmann, J. Appl. Crystallogr. 42 (2009) 339-341.

[18] G. Sheldrick, Acta Crystallogr Sect. A 64 (2008) 112-122.

[19] G. Sheldrick, Acta Crystallogr Sect. C 71 (2015) 3-8.

[20] C.F. Macrae, I.J. Bruno, J.A. Chisholm, P.R. Edgington, P. McCabe, E. Pidcock, L. Rodriguez-Monge, R. Taylor, J.v. Streek, P.A. Wood, J. Appl. Crystallogr. 41 (2008) 466-470.

[21] M. Nardelli, J. Appl. Crystallogr. 28 (1995) 659.

[22] A. Spek, Acta Crystallogr. Sect. D 65 (2009) 148-155.

[23] M. Frisch, G. Trucks, H. Schlegel, G. Scuseria, M. Robb, J. Cheeseman, G. Scalmani, V. Barone, B. Mennucci, G. Petersson, M. Nakatsuji, X. Li, H.P. Hratchian, A.F. Izmaylov, J. Bloino, G. Zheng, J.L. Sonnenberg, M. Hada, M. Ehara, K. Toyota, R. Fukuda, J. Hasegawa, M. Ishida, T. Nakajima, Y. Honda, O. Kitao, H. Nakai, T. Vreven, J.A. MontgomeryJr, J.E. Peralta, F. Ogliaro, M. Bearpark, J.J. Heyd, E. Brothers, K.N. Kudin, V.N. Staroverov, R. Kobayashi, J. Normand, K. Raghavachari, A. Rendell, J.C. Burant, S.S. Iyengar, J. Tomasi, M. Cossi, N. Rega, J.M. Millam, M. Klene, J.E. Knox, J.B. Cross, V. Bakken, C. Adamo, J. Jaramillo, R. Gomperts, R.E. Stratmann, O. Yazyev, A.J. Austin, R. Cammi, C. Pomelli, J.W. Ochterski, R.L. Martin, K. Morokuma, V.G. Zakrzewski, G.A. Voth, P. Salvador, J.J. Dannenberg, S. Dapprich, A.D. Daniels, Ö. Farkas, J.B. Foresman, J.V. Ortiz, J. Cioslowski, D.J. Fox, Gaussian 09, Revision A. 1 Gaussian, Inc.,, Wallingford, 2009, 2009.

[24] C. Møller, M.S. Plesset, Phys. Rev., 46 (1934) 618-622.

[25] S.F. Boys, F. Bernardi, Mol. Phys. 19 (1970) 553-566.

[26] R. Dennington, T. Keith, J. Millam, Semichem Inc., Shawnee Mission, KS (2009).

Highlights for the manuscript entitled "Can C–H···F–C hydrogen bonds alter crystal packing features in the presence of N–H···O=C hydrogen bond?"

- **Importance of fluorine mediated interactions in presence of strong hydrogen bond**
- **Synthesis and characterization of fluorinated amides**
- **Structural analysis using model molecular system**
- **Computational analysis of the strong and weak hydrogen bonds**
- **Crystal engineering using "organic fluorine"**